Monitoring peptide-surface interaction by means of molecular dynamics simulation

Nonella, M ; Seeger, S

Abstract: Protein adsorption and protein surface interactions have become an important research topic in recent years. Very recently, for example, it has been shown that protein clusters can undergo a surface-induced spreading after adsorption. Such phenomena emphasize the need of a more detailed insight into protein-silica interaction at an atomic level. Therefore, we have studied a model system consisting of a short peptide, a silica slab, and water molecules by means of classical molecular dynamics simulations. The study reveals that, besides of electrostatic interactions caused by the chosen charge distribution, the peptide interacts with the silica surface through formation of direct peptide-surface hydrogen bonds as well as indirect peptide-water-surface hydrogen bonds. The number of created hydrogen bonds varies considerably among the simulated structures. The strength of hydrogen bonding determines the mobility of the peptide on the surface and the internal flexibility of the adsorbed peptide.

DOI: https://doi.org/10.1016/j.chemphys.2010.10.005

Monitoring peptide-surface interaction by means of molecular dynamics simulation

Marco Nonella*, Stefan Seeger

Physikalisch-Chemisches Institut, Universität Zürich, Winterthurerstrasse 190, CH-8057 Zürich, Switzerland

Abstract

Protein adsorption and protein surface interactions have become an important research topic in recent years. Very recently, for example, it has been shown that protein clusters can undergo a surface-induced spreading after adsorption. Such phenomena emphasize the need of a more detailed insight into protein-silica interaction at an atomic level. Therefore, we have studied a model system consisting of a short peptide, a silica slab, and water molecules by means of classical molecular dynamics simulations. The study reveals that, besides of electrostatic interactions caused by the chosen charge distribution, the peptide interacts with the silica surface through formation of direct peptide-surface hydrogen bonds as well as indirect peptide-water-surface hydrogen bonds. The number of created hydrogen bonds varies considerably among the simulated structures. The strength of hydrogen bonding determines the mobility of the peptide on the surface and the internal flexibility of the adsorbed peptide.

Keywords: classical molecular dynamics simulation, hydrogen bonding, peptide-surface-interaction, flexibility of adsorbed peptides, lateral diffusion

1. Introduction

The interaction of small peptides or proteins with surfaces plays an important role in many areas of research. [1] For instance, protein adsorption occurs as a first step after

*Corresponding author. Fax: +41446356813, Phone +41446354450
Email addresses: mnonella@pci.uzh.ch (Marco Nonella), sseeger@pci.uzh.ch (Stefan Seeger)

integration of a biomedical implant device and, thus, affects the implants biocompatibility. [2] Upon getting in contact with the blood stream, adsorbed serum proteins can lead to thrombosis. [3]

Experimental investigations have made use of a large number of different surfaces, among them biological membranes as well as surface films like cellulose derivatives, poly-L-lysine, or activated silanes. For example, peptide-bilayer interactions have been investigated using various techniques such as NMR [4, 5], x-ray diffraction [6], or neutron diffraction. [7] Latour and coworkers have investigated adsorption processes for many years. Recently, they determined the adsorption free energy for peptide-surface interaction using SPR spectroscopy. [8, 9]

Various spectroscopic techniques such as NMR-, [10] IR-, [11], ATR-IR-spectroscopy [12], or SAF [13, 14, 15, 16] have been applied for investigating the interaction of proteins with silica surfaces. Based on IR spectroscopy, Basiuk et al., [17] suggested that glycine oligomer formation is catalyzed by the silica surface. An absorption band at 1760 cm^{-1} had been assigned to a silica-glycine anhydride which appears during such a reaction. Studies carried out by Lomenech at al. [18] and Meng et al. [19] however, did not find any covalent interaction between glycine and a silica surface. The latter work suggests that the adsorbed molecule interacts with the surface through the formation of specified hydrogen bonds, which give rise to small shifts of the infrared frequencies of the affected groups.

Although these studies provided much insight into protein-surface interaction in general, little information about the interactions at the atomic level could be gained. Computational studies are an attractive alternative to provide information at atomic detail. Thus, numerous computational studies of adsorption processes and adsorbate-surface interactions have been reported in the past. Depending on the size of the investigated systems, different levels of theory were applied. The interaction of L-Lysine with hydroxylated and functionalized quartz surfaces have been studied by Gambino et al. [20, 21] using classical and semi-empirical methods. According to the latter method the interaction between Lysine and surface silanol groups is mainly of electrostatic nature with some hydrogen bonding contribution, leading to short N - H $\cdots$ O - Si distances. The classical simulations point to the importance of solvation of surface and adsorbate. The binding

free energy of bovine Lactoferricin (LFCinB) with a palmitoyl-oleoyl-phosphatidylcholine (POPC) membrane was predicted by Vivcharuk et al. [22]. Furthermore MD simulations of peptide adsorption on various surfaces have, for example, also been carried out by Shepherd et al. [23], Raffaini and Ganazzoli [24], Chandrasekhar et al. [25], and Horineck et al. [26, 27]. Using the semi-empirical MOPAC method [28] thermodynamic properties of adsorbed residues [29] had been determined. By means of classical molecular dynamics method various types of solute-surface interactions [30, 31, 32] had been calculated. In the latter study hydrogen bonding is discussed in some detail. No direct peptide-surface hydrogen bonding had, however, been detected. Positively charged -NH_3^+ groups have found to interact with surface -COO^- groups only indirectly with two or three intervening water molecules. Correspondingly the peptide showed a certain amount of mobility over the surface. Besides of this electrostatic attraction, hydrophobic interactions between CH_2 groups of the peptide and CH_2 groups of the SAM surface had been found. Forte et al. [33] have investigated oligopeptide adsorption on a functionalized quartz surface. They have in detail studied the mobility of the adsorbed peptide in terms of variation of the dihedral angles Ψ and Φ. The dynamics of acridine orange at a $C_{8,18}$/water/acetonitrile interface was studied by means of molecular dynamics simulation [34]. From multiple 1 ns simulations, the diffusion coefficient of acridine orange in different water/acetonitrile mixtures was calculated. Moreover, averaged solvent densities were determined and the evolution of the acridine orange-surface distance during the simulations was monitored. Interestingly, it has been shown recently that protein clusters can be formed in solution before they adsorb on a surface. After adsorption, such clusters can undergo a surface-induced spreading. [13]

A detailed knowledge about peptide-surface at the molecular level is crucial for understanding such phenomena. Are peptides preferably interacting with a surface through direct or indirect interaction, i.e. mediated by water molecules? Is the conformational flexibility of a peptide affected through adsorption, i.e. could conformational changes be promoted in an adsorbed peptide? Are peptide-surface interactions long-living or are they broken and rebuild continuously? Is the phenomenon of surface-induced spreading as described in Ref. [13] made possible through short living, fluctuating peptide-surface interactions?

Theoretical methods like first-principles dynamics simulations or molecular dynamics simulations are well known methods for studying such problems and obtaining deeper insight into such systems at the atomic level. In a recent contribution we have carried out first principles dynamics simulations of an alanine-water-silica system [35]. We found that the amino acid interacts with the surface through direct hydrogen bonds as well as through indirect amino acid-water-silanol hydrogen bonds. In these simulations, we have not found any evidence for a formation of a covalent alanine-silica bond. The finding of only non-covalent amino acid-surface interactions is important and justifies the use of a classical force field for the simulation of peptide-silica systems.

In this contributions we apply classical molecular dynamics in order to answer some of the raised questions. In the first part, we study spontaneous adsorption of a ALA-LYS-LYS-LYS-ALA peptide on a silica slab immersed in a box of water. Spontaneous adsorption is facilitated through the chosen simulation conditions between neutral and physiological pH which renders the silica surface negatively and the peptide positively charged, i.e. the surface carries a charge of -19 and the peptide one of +3. The peptide was placed in different orientations above the surface and its movement towards the surface was monitored as well as the formation of direct and indirect hydrogen bonds between the peptide and the surface. These simulations were first run for 1 ns. Subsequently, they were extended by additional 20 ns followed by 1 ns for a second analysis.

In the second part adsorption was enforced using steered molecular dynamics (SMD) [36] followed by an equilibration. This procedure leads to peptide-surface complexes located in the vicinity of the center of the slab and facilitates the formation of structures exhibiting strong peptide-surface interaction. After equilibration the dynamics of the adsorbed peptide was studied during 1 ns. Subsequently, a second equilibration of 20 ns was carried out, followed by a 1 ns trajectory for analysis.

2. Computational Methods

2.1. Generation of the simulation systems

As suggested by Civalleri et al. [37] we have used the edingtonite structure to model a silica surface. In order to have a proper building block for generating silica slabs, the geometry of a fully saturated structural unit of edingtonite was optimized at the

B3LYP/6-31G* level of theory [38, 39, 40] using the GAUSSIAN03 suite of programs [41]. Using this method, also atomic partial charges of an edingtonite structure were determined by means of the CHELPG method. [42] The obtained partial charges could in very good approximation be simplified to +1.6 for Si, -0.8 for O and +0.4 for H in the case of saturated silanol groups. By computing vibrational frequencies of a chromophore embedded in a solvent [43, 44] or a protein [45] we have demonstrated that with a CHARMM force field for one part of a simulated system and CHELP charges for the other part very satisfactory results can be obtained. The CHARMM22 force field [46] was applied for the peptide and TIP3P parameters were used for water molecules [47]. In order to run silica-water-peptide simulation, also non-bonded parameter for silica-water and silica-peptide interactions have to defined.

In order to construct a bonded edingtonite force field we choose to follow a similar approach as described in Ref. [48] We have taken the force field developed by Hill and Sauer [49] and have fitted to their potentials harmonic potentials using the program Grace. Since in a CHARMM-type force field [50] van der Waals interactions are represented through a Lennard-Jones 6-12 potential, two adjustable parameters, namely σ_{ij}, denoting the distance between atoms i and j and ϵ_{ij}, denoting the interaction energy of atoms i and j at equilibrium distance σ_{ij}, have to be determined. In CHARMM-type force fields, r_{ij} and ϵ_{ij} are determined from atom type based properties using the combination rules:

$$\sigma_{ij} = \frac{\sigma_{ii} + \sigma_{jj}}{2}$$

and

$$\epsilon_{ij} = \sqrt{\epsilon_{ii} \cdot \epsilon_{jj}}$$

This leaves us with the problem of finding a suitable set of ϵ and σ parameters for the atoms involved in the silica part of our simulation system. Since non-bonded interactions between atoms belonging to the slab have been excluded in our setup and since the surface of our slab is covered with silanol or deprotonated silanol groups, hereby generating a highly hydrophilic surface, the key terms we have to define are the ϵ and σ values for the silanol oxygen and proton as well as for the dangling oxygens. For both oxygen atoms,

we have taken the hydroxyl oxygen parameters from the CHARMM force field and for the silanol proton the corresponding parameters of the hydroxyl proton (σ_O = 2.8509 Å, ϵ_O = 0.1591 kcal/mol, σ_H = 1.4254 Å, ϵ_H = 0.0498 kcal/mol). Furthermore, parameters for silica atoms have been derived as follows: a B3LYP/6-31G** calculation of a $SiO_2 \cdots H_2O$ complex revealed an Si-O distance of about 1.94 Å and an interaction energy of about -126 kJ/mol. Compromising between atom distance and interaction energy led us to choose a σ_{Si} of 3.20 Å and an ϵ_{Si} of 0.100 kcal/mol. The latter two parameters differ considerably from those of Ref. [48] (σ_{Si} =3.826, ϵ_{Si} = 0.30 kcal/mol) which were obtained using a different procedure. Van der Waals interactions were treated using a force-switching method with a cutoff of 16.0 and a switching distance of 14.0 Å. For the description of electrostatic interactions, the Particle Mesh Ewald method [51] was applied.

We have tested our force field by minimizing the three structures depicted in Figure 1. Structure a) corresponds to a completed, fully saturated edingtonite unit, and Structure b) represents the building block which is used for generating a three dimensional slab. Both structures were minimized using X-PLOR [52] and revealed RMS deviations from the quantum chemically optimized fully saturated edingtonite structure of 0.42 and 0.21, respectively. Structure c), a slab of 147 edingtonite units (7 x 7 x 3), was minimized using NAMD [53]. For this minimization, periodic boundary conditions had been applied. Despite the fact that NAMD cannot deal with periodic boundaries through covalent bonds, the structure of this slab was well retained with the final set of parameters showing an overall deviation from the starting structure with an RMS value of 0.22 Å. Not surprisingly, the largest deviations were found at the borders of the slab. Since we are focussing mainly on peptide-surface interaction in the vicinity of the center of the slab surface, the effect of these structural deficiencies should be negligible. In all following steps, except during one short minimization, all or a part of the slab atoms were subject to harmonic constraints. Due to the applied constraints as well as due to the three-dimensional network of the SiO_2 structure, involved atoms are considerably restricted in their ability to move, i.e. conformational changes within the silica slab are prevented. Therefore we consider our method of parameter testing as sufficient. This assumption was confirmed by finding only weak distortions of the surface in all simulations. Therefore, we

conclude that our set of parameters is capable to reproduce the slab structure sufficiently accurate for our purpose.

In order to prepare the silica slab for our final simulation system, we proceeded as follows: the same slab that was used for parameter optimizing and testing was fully covered with silanol groups on top and bottom and immersed in a water box. The system was then subject to a short full minimization followed by an equilibration at 300K. During the equilibration all atoms belonging to the slab were constrained in their ability to move.

For quartz surfaces a pK_a of about 7.5 had been determined for terminal silanol groups [54]. In the range between neutral pH and a physiological pH of 7.4, between about a third and half of the silanol groups are thus assumed to be deprotonated. We have, therefore, deprotonated silanol groups of the top layer of the equilibrated slab randomly such that approximately 50% of the silanol groups of the top layer were deprotonated, leading to a slab with a charge of -19.0. For all following simulations, the atoms of the lowest of the three edingtonite layers were constrained in their ability to move by applying harmonic constraints.

The such way prepared slab was immersed in a water box, an ALA-LYS-LYS-LYS-ALA peptide was placed in random orientation above the slab such that the distance between slab and C_α-atom of the central lysine was about 35 Å. The lysine side chain has a pK_a of about 10.5. Under the conditions of interest, LYS is thus positively charged and our peptide has a total charge of +3. In order to set the total charge of the simulation system to zero, Cl^- and Na^+ ions were added such that the ionic strength was about 0.15 mol/l. All simulations were started with a linear peptide as shown in Figure 2.

Finally, water molecules within a distance of 2.5 Å of the slab, the alanine, or of the ions were cut out. This setup was carried out using the programs X-PLOR [52] and VMD [55], ions were added using the autoionize plugin within VMD. The resulting system contains 147 edingtonite units, a peptide, 8430 water molecules, 3 chlorides, and 19 sodium ions which, after completed equilibration, were allowed to move freely.

This system was minimized and equilibrated at 300K applying a Langevin thermostat. Hereby, the pressure of the system was adjusted to 1 atm applying a Langevin piston technique [56]. This procedure resulted in a box of the size of 51.0 Å x 54.5 Å x 101.5 Å.

The large z-dimension had been chosen in order to minimize artifacts due to the fact that NAMD can only handle three-dimensional periodic systems. The such way adjusted box was then kept fix in the following simulations, i.e. these simulations were then carried out in the NVT-ensemble.

The computed trajectories were analyzed using the programs VMD [55] and X-PLOR. For calculating lateral and vertical diffusion coefficients, trajectories were converted and read into GROMACS [57, 58, 59].

3. Results and Discussion

3.1. Spontaneous adsorption

Our setup leads to strong electrostatic surface-peptide interactions. This should allow to study free adsorption within reasonable simulation times. We have carried out ten such simulations, starting each time with a differently orientated peptide about 35 Å above the surface, using a pre-equilibrated structure. After placing the peptide, an additional short equilibration of 50 ps had been run during which the C_α-atom of the central lysine was restrained by a harmonic potential. This equilibration was then followed by 1 ns of free dynamics simulation.

Despite the strong electrostatic surface-peptide interaction, the pathway of adsorption very much depends on the original orientation of the peptide and the structure achieved after equilibration. Two prototypical examples of free adsorption simulations (simulations a and b) are now discussed in some detail. Taking the z-coordinate of the C_α-atom of the central lysine as observable, a smooth and steady approach of the peptide is only rarely observed. Figure 3 depicts how the z-coordinate varies with time (top) and the hereby involved lateral diffusion (bottom).

While in simulation a) a close contact with the surface is established already after about 0.4 ns, in simulation b) this is achieved only towards the end of the 1 ns simulation time. Also, lateral diffusion extends over a larger area in simulation b) than in a). In case b), this causes adsorption far away from the center of the slab in the vicinity of its border.

Our primary interest focusses on the detailed interactions between peptide and surface. On the level of our applied force field, these interactions consist of electrostatic and

van der Waals energies. Applying geometrical rules, the formation of hydrogen bonds can be monitored. Figure 4 shows the number of direct (top) and indirect (middle, hydrogen bonds slab-water-peptide) hydrogen bonds that were formed between slab and peptide during the spontaneous adsorption. The bottom graphs of Figure 4 finally show electrostatic, van der Waals, and total interaction energies between slab and peptide. These energies have been calculated using X-PLOR [52]. For calculation of the non-bonding interaction energies a cutoff of 12 Å was applied. For van der Waals interaction, a switching method was used which starts to become effective at 11 Å. Electrostatic potentials were shifted. Figures 3 and 4 demonstrate that even in the presence of strong electrostatic interactions, the adsorption pathways can vary considerably.

After this first analysis we have continued the simulation for 20 ns, followed by 1 ns for analysis. We now find an increase of direct and indirect hydrogen bonds in both simulations as depicted in Figure 5. Simulation a) still exhibits more peptide-surface hydrogen bonds than simulation b). Based on this data it can still not be decided whether equilibrated structures have been attained. It is, however, not the aim of the present work to give an estimate for the time needed in order to accomplish an equilibrium distribution of adsorbed peptides. Instead we focus on peptide-surface interaction and internal flexibility of adsorbed peptides which we discuss in Section 3.2.

3.2. Free dynamics after enforced adsorption

In several simulations dicussed in section 3.1, the adsorbed peptide was found near the border of the slab. As discussed in section 2, periodicity is only to some extend accounted for in our setup. Therefore, the region around the center of the slab provides a better physical description of an adsorbed peptide. Moreover, adsorbed structures at thermal equilibrium might only be achieved after much longer simulation times than we have carried out in the previous section. Therefore, we have applied a different approach for studying the behavior of the adsorbed peptide.

We enforced adsorption using steered molecular dynamics (SMD) [60, 36]. By applying a force to the C_α-atom of the central lysine, the peptide was pulled towards the slab with a constant velocity of 0.001 Å/fs. This simulation was run for 50 ps in order to ensure to end up with a strongly adsorbed protein. After this enforced adsorption

the steering force was removed and a free equilibration was run for 1 ns followed by a simulation of 1 ns duration for analysis.

As before, we have analyzed the number of direct and indirect peptide-layer hydrogen bonds, lateral and vertical movement of the peptide, interaction energies peptide-layer, as well as the behavior of the peptides Φ and Ψ dihedral angles.

Ten trajectories were analyzed in detail and showed a large variety concerning peptide-surface interaction or internal flexibility of the peptide. For instance, there is one simulation where we find up to five direct hydrogen bonds and another one which exhibits up to five indirect hydrogen bonds. In both cases, strong peptide-layer interactions must exist. Such strongly interacting structures are shown in Figure 6. The snapshot at the top shows a structure with five direct peptide-surface hydrogen bonds whereas the one at the bottom shows a structure with five indirect peptide-water-surface hydrogen bonds. In none of our trajectories more than five direct or indirect hydrogen bonds could be found.

All the direct hydrogen bonds are Lys-NH_3^+ $\cdots$ O-Si interactions whereas different types of interactions are found in case of the indirect hydrogen bonds: these interactions are either of a type N-H $\cdots$ O-H $\cdots$ O-Si or N-H $\cdots$ O $\cdots$ H-O-Si. The N-H group can either belong to a Lysine -NH_3^+ group, to a peptide N-H moiety, or to the terminal ammonium group.

In many structures, between one and three hydrogen bonds of each type have been found. Typical patterns of number of hydrogen bonds are depicted in Figure 7. The two plots on the top show trajectories with either many direct or indirect hydrogen bonds, the two graphs at the bottom show two trajectories with only few direct or indirect such interactions. Even in the presence of strong attractive interactions between surface and peptide, hydrogen bonds are continuously formed and broken during the trajectories as is demonstrated in Figure 7. From these observations a certain mobility of the adsorbed peptide must be assumed.

After this first analysis we have continued to simulate each structure for 20 ns, followed by 1 ns for a second analysis. From the analysis of the hydrogen bonding patterns, it is evident, that conformational changes occurred during these simulations. Structures which showed many hydrogen bonds during the first analysis show now considerably less

and vice versa. In a recent study on the properties of leucine-enkephaline adsorbed on a membrane using NMR spectroscopy and molecular dynamics simulations it was found that an adsorbed peptide is flexible and switches between conformations. [25]. Thus, we can assume that an ensemble of different adsorbed structures exists.

We have inspected all trajectories for the existence of structures exhibiting one or two direct or indirect hydrogen bonds for both periods of analysis. That way we can determine probability distributions for finding a certain type of hydrogen bond as shown in Figure 8. The distributions derived from the two analyzed periods of the trajectory agree quite well; although it must be realized, that the small ensemble size causes broad distributions. However, the maximum of all distributions determined using the set of trajectories after 20 ns of equilibration are found slightly moved to the left compared to those arising from the first analysis period. After the additional equilibration we thus find a slightly less number of structures exhibiting peptide-surface hydrogen bonding. From these findings we conclude that the 1 ns equilibration after enforced adsorption was too short in order to reach an equilibrated ensemble of peptide-surface structures. We might even suggest, that such distributions might serve as a criteria in order to decide whether such an ensemble is in a thermal equilibrium.

A quantification of the peptide's mobility can be achieved from a simulation through the determination of diffusion coefficients. Hereby, a common problem is the time scale. Simulations are rarely longer than a few tens of nanoseconds while experiments are carried out on much longer time scales. In the past, diffusion coefficients have been determined from MD simulations using trajectories with simulation times from about 400 ps [61] to several nanoseconds [62, 63, 64, 65]. For our system, the simulation time of only 1 ns can only be expected to reveal diffusion coefficients containing a very large uncertainty. Averaging over ten trajectories should, however, improve the determined values. After averaging we find a lateral diffusion coefficient of $0.010 \pm 0.016 \cdot 10^{-5}$ cm^2/s for the lateral movement and a vertical diffusion coefficient of $0.005 \pm 0.006 \cdot 10^{-5}$ cm^2/s for the vertical movement. For comparison we have run a 1 ns simulation of the same peptide in a water box which revealed a diffusion coefficient of $0.24 \pm 0.02 \cdot 10^{-5}$ cm^2/s. In order to check whether such a relatively short trajectory can provide a reasonable diffusion coefficient, we need to compare our result to experimental data. Due

to the lack of such data for our peptide, we compare the result of our simulation with the experimental diffusion coefficients of sucrose ($0.52 \cdot 10^{-5}$ cm^2/s), glucose ($0.67 \cdot 10^{-5}$ cm^2/s), and alanine ($0.91 \cdot 10^{-5}$ cm^2/s)[66] which are all smaller than our peptide and, therefore, should indeed possess a larger diffusion coefficient. In contrast, the much larger macromolecule poly-l-lysine with an average molecular weight of 230500 Da exhibits a considerably smaller diffusion coefficient of $4.0 \pm 0.5 \cdot 10^{-9}$ cm^2/s) [67]. From that comparison, we conclude, that the outcome of our simulation is reasonable enough for a qualitative discussion.

After having discussed the mobility of the peptide as an entity we now focus on the internal flexibility. The internal dynamics is best analyzed by monitoring the variation of the dihedral angles Φ and Ψ. The respective dihedrals are indicated in Figure 2. We only discuss a selection of typical trajectories and only depict those dihedrals which, in some of the trajectories, undergo some changes. For instance, in the simulation which exhibited the strongest direct h-bonds (see Figure 6, top) only minute variations are found in all dihedrals (Figure 9 a). On the contrary, the simulation exhibiting only few direct h-bonds (see Figure 7 c) undergoes larger conformational changes (Figure 9 b). In some of the trajectories, alterations are found that last only for a very short time like that for Ψ_4 in Figure 9 c) and d) while in others, like that in the case of Ψ_3 in Figure 9 e), a new conformation is attained which seems to be stable on the timescale of the simulation. For comparison, the time development of the same dihedrals during a 1 ns simulation of the peptide in a water box is shown in Figure 9 f. Accordingly, the peptide-surface interaction seems not to confine the internal flexibility of the peptide and, occasionally, might even promote conformational changes. Similar conformational changes are also found during the analysis after the additional equilibration. In four of the ten structures larger conformational changes occur in one or two dihedrals. This flexibility could be an implication of still not equilibrated systems. It could, however, as well hint towards a certain flexibility of the adsorbed peptide in agreement with the findings of Chandrasekhar et al. [25].

4. Conclusion

In the first part of this study we have presented results from free adsorption simulations of a short peptide onto a silica surface. The strong electrostatic attraction which results from a negatively charged surface and a positively charged peptide gives rise to spontaneous adsorption. Pathways and velocities of the adsorption processes differed for different starting conditions. However, within a simulation time of 22 ns, the systems might still not have reached thermal equilibrium.

Therefore, in the second part, we have generated structures exhibiting strong peptide-surface interactions by means of SMD simulation. After enforced adsorption followed by an equilibration, structures were simulated during 1 ns for anaylsis. In agreement with previously carried out quantum chemical simulations [35], peptide-surface interactions occur through direct and indirect hydrogen bonds. Both these interactions are continuously broken and rebuilt during a trajectory, i.e. the achieved 'adsorbed state' is by no means static but shows strong dynamical features. Besides of the dynamical nature of peptide-surface hydrogen bonds, the adsorbed peptides exhibit a certain lateral diffusion as well as some internal flexibility. The first observation we have quantified in terms of lateral diffusion coefficients and the latter is documented by monitoring the behavior of the torsional angles Ψ and Φ. On the time scale of our simulations, the achieved structures of surface-water-peptide complexes are all different. Nevertheless, the dynamical behavior of the dihedrals Ψ and Φ show a similar pattern. An extension of the simulation time up to 20 ns may hint towards some further relaxation of the simulation systems which is manifested in a slightly smaller number of structures showing direct or indirect peptide-surface hydrogen bonding than during the first period of analysis. On the other hand, similar configurational changes of the peptide are found in both parts of the trajectories used for analysis.

5. Acknowledgment

Computations were performed on the Matterhorn and Schrödinger Clusters of the University of Zurich. We thank J. Robert Huber for critically reading the manuscript. Financial support by Schweizerischer Nationalfonds (SNF) is gratefully acknowledged.

References

[1] J. J. Gray, Cur. Opin. Struct. Biol. 14 (2004) 110–115.

[2] J. D. Andrade, V. Hlady, Adv. Polym. Sci. 79 (1986) 1–63.

[3] R. K. Walker, S. Krishnawamy, J. Biol. Chem. 269 (1994) 27441–27450.

[4] S. J. Opella, Nat. Struct. Biol. 4 Suppl. (1997) 845–8.

[5] R. B. Klassen, S. J. Opella, Methods Mol Biol 60 (1997) 271–97.

[6] B. A. Wallace, R. W. Janes, Journal of Molecular Biology 217 (1991) 625 – 627.

[7] R. E. Jacobs, S. H. White, Biochemistry 28 (1989) 3421–3437.

[8] Y. Wei, R. A. Latour, Langmuir 24 (2008) 6721–6729.

[9] Y. Wei, R. A. Latour, Langmuir 25 (2009) 5637–5646.

[10] J. R. Long, W. J. Shaw, P. S. Stayton, G. P. Drobny, Biochemistry 40 (2001) 15451 – 15455.

[11] Y. I. Tarasevich, L. I. Monakhova, Colloid J. 64 (2002) 482–487.

[12] C. E. Giacomelli, M. G. E. G. Bremer, W. Norde, J. Colloid Interface Sci. 220 (1999) 13–23.

[13] M. Rabe, D. Verdes, S. Seeger, Soft Matter 5 (2009) 1039–1047.

[14] M. Rabe, D. Verdes, M. Rankl, G. R. J. Artus, S. Seeger, ChemPhysChem 8 (2007) 862–72.

[15] M. Rabe, D. Verdes, J. Zimmermann, S. Seeger, J Phys Chem B 112 (2008) 13971–13980.

[16] M. Rankl, T. Ruckstuhl, M. Rabe, G. R. J. Artus, A. Walser, S. Seeger, ChemPhysChem 7 (2006) 837–846.

[17] V. A. Basiuk, T. Y. Gromovoy, V. G. Golovaty, A. M. Glukhoy, Origins of Life and Evolution of Biospheres 20 (1990) 483–498.

[18] C. Lomenech, G. Bery, D. Costa, L. Stievano, J. F. Lambert, ChemPhysChem 6 (2005) 1061–1070.

[19] M. Meng, L. Stievano, J.-F. Lambert, Langmuir 20 (2004) 914–923.

[20] G. L. Gambino, G. M. Lombardo, A. Grassi, G. Marletta, J. Phys. Chem. B 108 (2004) 2600–2607.

[21] G. L. Gambino, A. Grassi, G. Marletta, J. Phys. Chem. B 110 (2006) 4836–4845.

[22] V. Vivcharuk, B. Tomberli, I. S. Tolokh, C. G. Gray, Phys. Rev. E. Stat. Nonlin. Soft Matter Phys. 77 (2008) 031913.

[23] C. M. Shepherd, K. A. Schaus, H. J. Vogel, A. H. Juffer, Biophys J 80 (2001) 579–596.

[24] G. Raffaini, F. Ganazzoli, Langmuir 20 (2004) 3371 – 3378.

[25] I. Chandrasekhar, W. F. van Gunsteren, G. Zandomeneghi, P. T. F. Williamson, B. H. Meier, J Am Chem Soc 128 (2006) 159–70.

[26] D. Horinek, A. Serr, M. Geisler, T. Pirzer, U. Slotta, S. Q. Lud, J. A. Garrido, T. Scheibel, T. Hugel, R. R. Netz, Proc. Natl. Acad. Sci. USA 105 (2008) 2842–2847.

[27] A. Serr, D. Horinek, R. R. Netz, J. Am. Chem. Soc. 130 (2008) 12408–12413.

[28] J. J. Stewart, J. Comput. Aided Mol. Des. 4 (1990) 1–105.

[29] R. A. Latour, L. L. Hench, Biomaterials 23 (2002) 4633–4648.

[30] Y. Sun, R. A. Latour, Journal of Computational Chemistry 27 (2006) 1908–1922.

[31] F. Wang, S. J. Stuart, R. A. Latour, Biointerphases 3 (2008) 9 – 18.

[32] V. P. Raut, M. A. Agashe, S. J. Stuart, R. A. Latour, Langmuir 21 (2005) 1629 – 1639.

[33] G. Forte, A. Grassi, G. Marletta, J. Phys. Chem. B. 111 (2007) 11237–43.

[34] A. Fouqueau, M. Meuwly, R. J. Bemish, J Phys Chem B 111 (2007) 10208–16.

[35] M. Nonella, S. Seeger, ChemPhysChem 9 (2008) 414–421.

[36] B. Isralewitz, J. Baudry, J. Gullingsrud, D. Kosztin, K. Schulten, J. Mol. Graphics Modell. 19 (2001) 13.

[37] B. Civalleri, S. Casassa, E. Garrone, C. Pisani, P. Ugliengo, J. Phys. Chem. B 103 (1999) 2165–2171.

[38] A. D. Becke, J. Chem. Phys 98 (1993) 5648–5652.

[39] P. J. Stephens, F. J. Devlin, C. F. Chabalowski, M. J. Frisch, J.Phys.Chem. 98 (1994) 11623–11627.

[40] M. Francl, W. Pietro, W. Hehre, J. Binkley, M. Gordon, D. deFrees, J. Pople, J. Chem. Phys. 77 (1982) 3654–3665.

[41] M. J. Frisch, G. W. Trucks, H. B. Schlegel, G. E. Scuseria, M. A. Robb, J. R. Cheeseman, J. A. Montgomery, Jr., T. Vreven, K. N. Kudin, J. C. Burant, J. M. Millam, S. S. Iyengar, J. Tomasi, V. Barone, B. Mennucci, M. Cossi, G. Scalmani, N. Rega, G. A. Petersson, H. Nakatsuji, M. Hada, M. Ehara, K. Toyota, R. Fukuda, J. Hasegawa, M. Ishida, T. Nakajima, Y. Honda, O. Kitao, H. Nakai, M. Klene, X. Li, J. E. Knox, H. P. Hratchian, J. B. Cross, V. Bakken, C. Adamo, J. Jaramillo, R. Gomperts, R. E. Stratmann, O. Yazyev, A. J. Austin, R. Cammi, C. Pomelli, J. W. Ochterski, P. Y. Ayala, K. Morokuma, G. A. Voth, P. Salvador, J. J. Dannenberg, V. G. Zakrzewski, S. Dapprich, A. D. Daniels, M. C. Strain, O. Farkas, D. K. Malick, A. D. Rabuck, K. Raghavachari, J. B. Foresman, J. V. Ortiz, Q. Cui, A. G. Baboul, S. Clifford, J. Cioslowski, B. B. Stefanov, G. Liu, A. Liashenko, P. Piskorz, I. Komaromi, R. L. Martin, D. J. Fox, T. Keith, M. A. Al-Laham, C. Y. Peng, A. Nanayakkara, M. Challacombe, P. M. W. Gill, B. Johnson, W. Chen, M. W. Wong, C. Gonzalez, J. A. Pople, Gaussian 03, Revision C.02, 2004. Gaussian, Inc., Wallingford, CT.

[42] C. M. Breneman, K. B. Wiberg, J. Comp. Chem. 11 (1990) 361–373.

[43] M. Klähn, G. Mathias, C. Kötting, M. Nonella, J. Schlitter, K. Gerwert, P. Tavan, The Journal of Physical Chemistry A 108 (2004) 6186–6194.

[44] M. Nonella, G. Mathias, P. Tavan, The Journal of Physical Chemistry A 107 (2003) 8638–8647.

[45] M. Nonella, G. Mathias, M. Eichinger, P. Tavan, The Journal of Physical Chemistry B 107 (2003) 316–322.

[46] A. D. MacKerell, D. Bashford, Bellott, R. L. Dunbrack, J. D. Evanseck, M. J. Field, S. Fischer, J. Gao, H. Guo, S. Ha, D. Joseph-McCarthy, L. Kuchnir, K. Kuczera, F. T. K. Lau, C. Mattos, S. Michnick, T. Ngo, D. T. Nguyen, B. Prodhom, W. E. Reiher, B. Roux, M. Schlenkrich, J. C. Smith, R. Stote, J. Straub, M. Watanabe, J. Wiorkiewicz-Kuczera, D. Yin, M. Karplus, The Journal of Physical Chemistry B 102 (1998) 3586–3616.

[47] W. L. Jorgensen, J. Chandrasekhar, J. D. Madura, R. W. Impey, M. L. Klein, J. Chem. Phys. 79 (1983) 926–935.

[48] E. R. Cruz-Chu, A. Aksimentiev, K. Schulten, J. Phys. Chem. B 110 (2006) 21497–21508.

[49] J. Hill, J. Sauer, J. Phys. Chem. 98 (1994) 1238–1244.

[50] B. R. Brooks, R. E. Bruccoleri, D. J. Olafson, D. J. States, S. Swaminathan, M. Karplus, Journal of Computational Chemistry 4 (1983) 187–217.

[51] T. Darden, D. York, L. Pedersen, The Journal of Chemical Physics 98 (1993) 10089–10092.

[52] A. T. Brünger, in: N. W. Isaacs, M. R. Taylor (Eds.), Crystallographic computing 4: Techniques and new technologies, Clarendon Press, Oxford, 1988.

[53] J. C. Phillips, R. Braun, W. Wang, J. Gumbart, E. Tajkhorshid, E. Villa, C. Chipot, R. D. Skeel, L. Kale, K. Schulten, Journal of Computational Chemistry 26 (2005) 1781–1802.

[54] W. A. House, D. R. Orr, J. Chem. Soc. Faraday Trans. 88 (1992) 233 – 241.

[55] W. Humphrey, A. Dalke, K. Schulten, Journal of Molecular Graphics 14 (1996) 33–38.

[56] G. J. Martyna, D. J. Tobias, M. L. Klein, J. Chem. Phys. 101 (1994) 4177–418.

[57] D. van der Spoel, A. R. van Buuren, E. Apol, P. J. Meulenhoff, D. P. Tieleman, A. L. T. M. Sijbers, B. Hess, K. A. Feenstra, E. Lindahl, R. van Drunen, H. J. C. Berendsen, Gromacs User Manual version 3.1, Nijenborgh 4, 9747 AG Groningen, The Netherlands. Internet: http://www.gromacs.or, 2001.

[58] H. J. C. Berendsen, D. van der Spoel, R. van Drunen, Comp. Phys. Comm. 91 (1995) 43–56.

[59] E. Lindahl, B. Hess, D. van der Spoel, J. Mol. Mod. 7 (2001) 306–317.

[60] B. Isralewitz, M. Gao, K. Schulten, Curr. Opin. Struct. Biol. 11 (2001) 224.

[61] P. Liu, E. Harder, B. J. Berne, The Journal of Physical Chemistry B 108 (2004) 6595–6602.

[62] H. Higashi, T. Oda, Y. Iwai, Y. Arai, Fluid Phase Equilibria 219 (2004) 55 – 60.

[63] H. Higashi, Y. Iwai, , Y. Arai, Ind. Eng. Chem. Res. 39 (2000) 4567 – 4570.

[64] Y. Iwai, H. Higashi, H. Uchida, Y. Arai, Fluid Phase Equilibria 127 (1997) 251 – 261.

[65] K. K. Burusco, C. Jaime, F. Franch-Lage, L. Beltran, F. Granero, JOURNAL OF THE AMERICAN OIL CHEMISTS SOCIETY 87 (2010) 271–279.

[66] D. R. Lide, Handbook of Chemistry and Physics, CRC Press, Inc., Boca Raton, 76th edition edition, pp. 8–64.

[67] L. Rodríguez-Maldonado, A. Fernández-Nieves, A. Fernández-Barbero, Colloids and Surfaces A 270-271 (2005) 335 – 339.

List of Figures

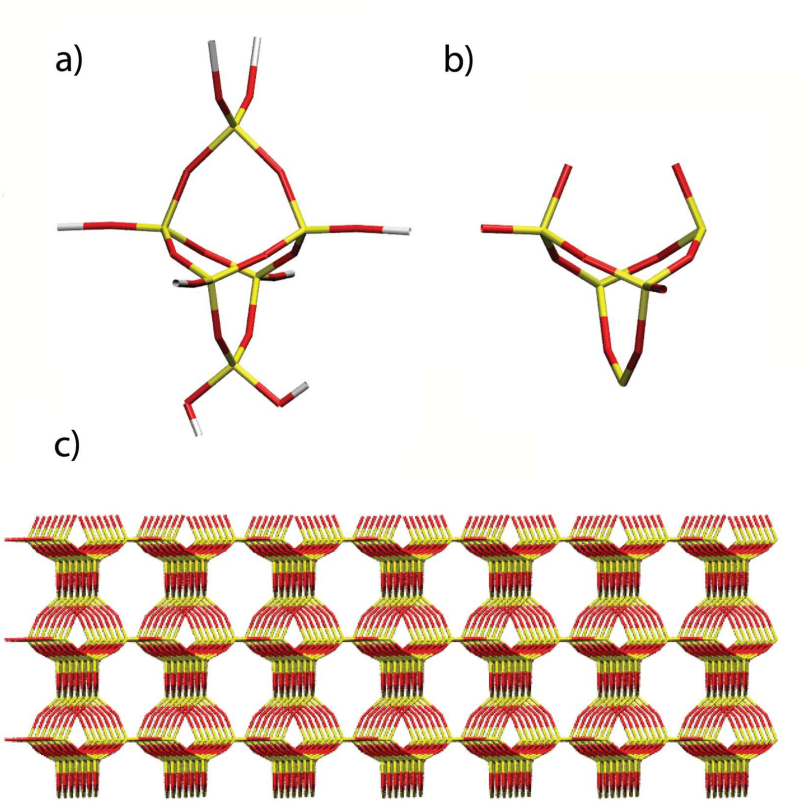

Figure 1: Structures used for optimizing and testing the force field. Atoms are colored as follows: oxygen: red, silicon: yellow, hydrogen: white.

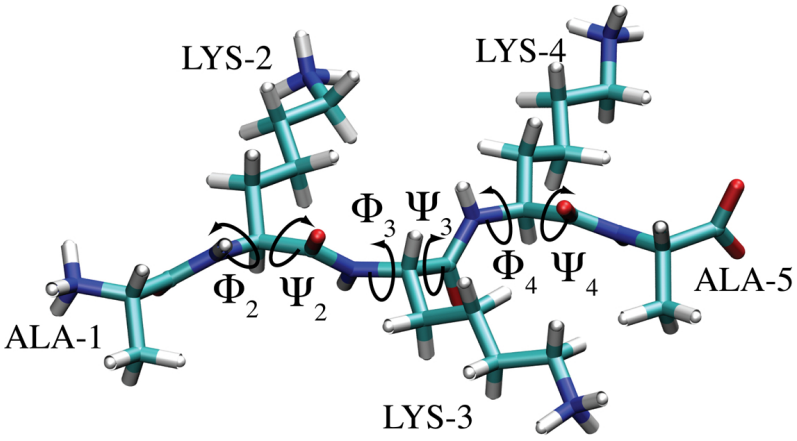

Figure 2: Structure of the ALA-LYS-LYS-LYS-ALA peptide at the beginning of the simulations. Included are the labels for the dihedral angles Φ and Ψ.

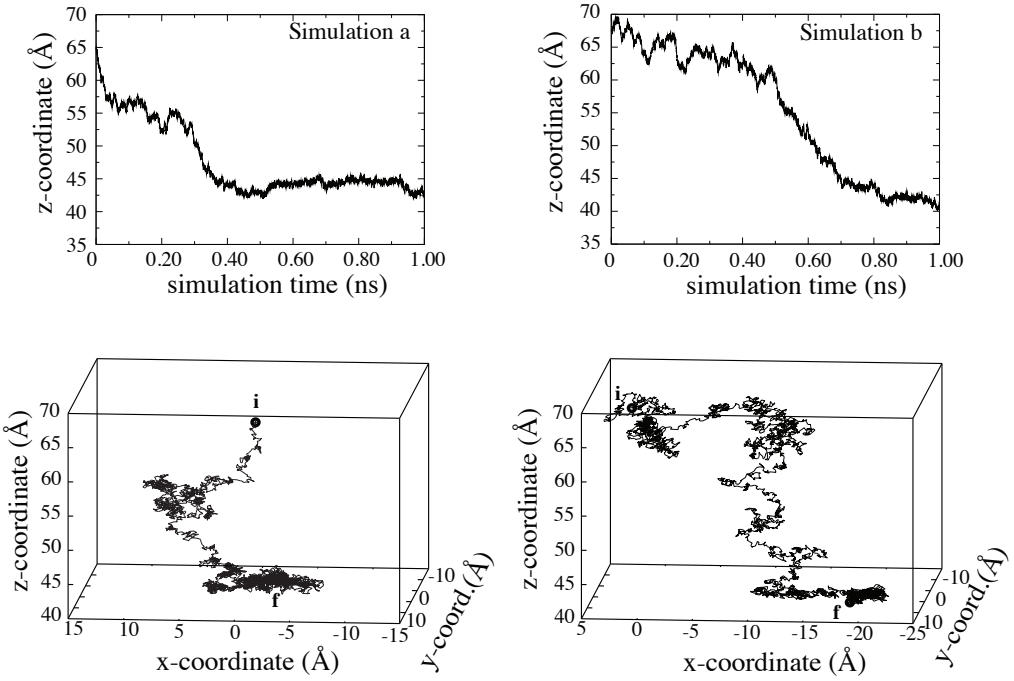

Figure 3: Upper part: Movement of the C^{α} of the central lysine in z-direction. Lower part: Lateral displacement of the same atom as a function of the z-coordinate.

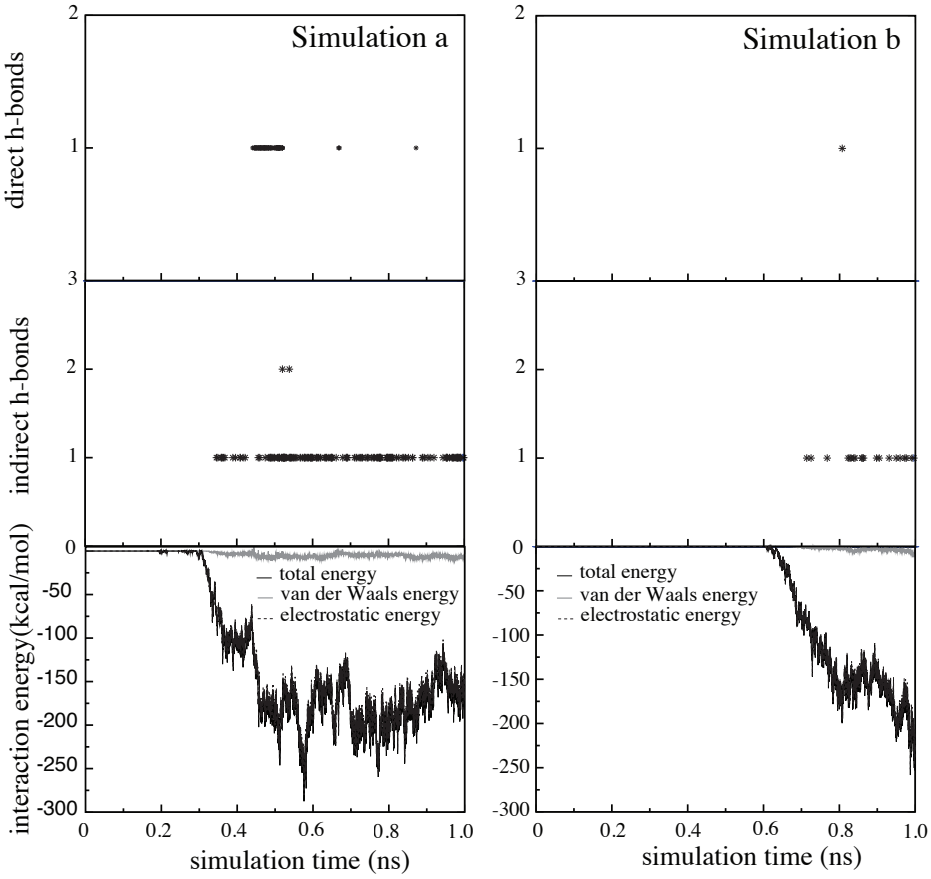

Figure 4: Direct (top) and indirect (middle) hydrogen bonds and interaction energies between peptide and surface (bottom)

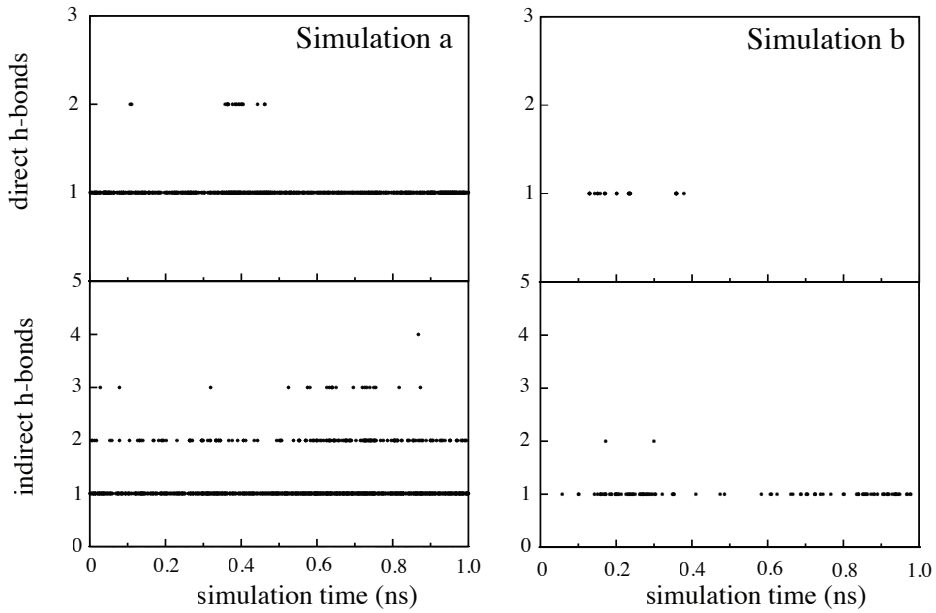

Figure 5: Direct (top) and indirect (bottom) hydrogen bonds after additional free dynamics of 20 ns.

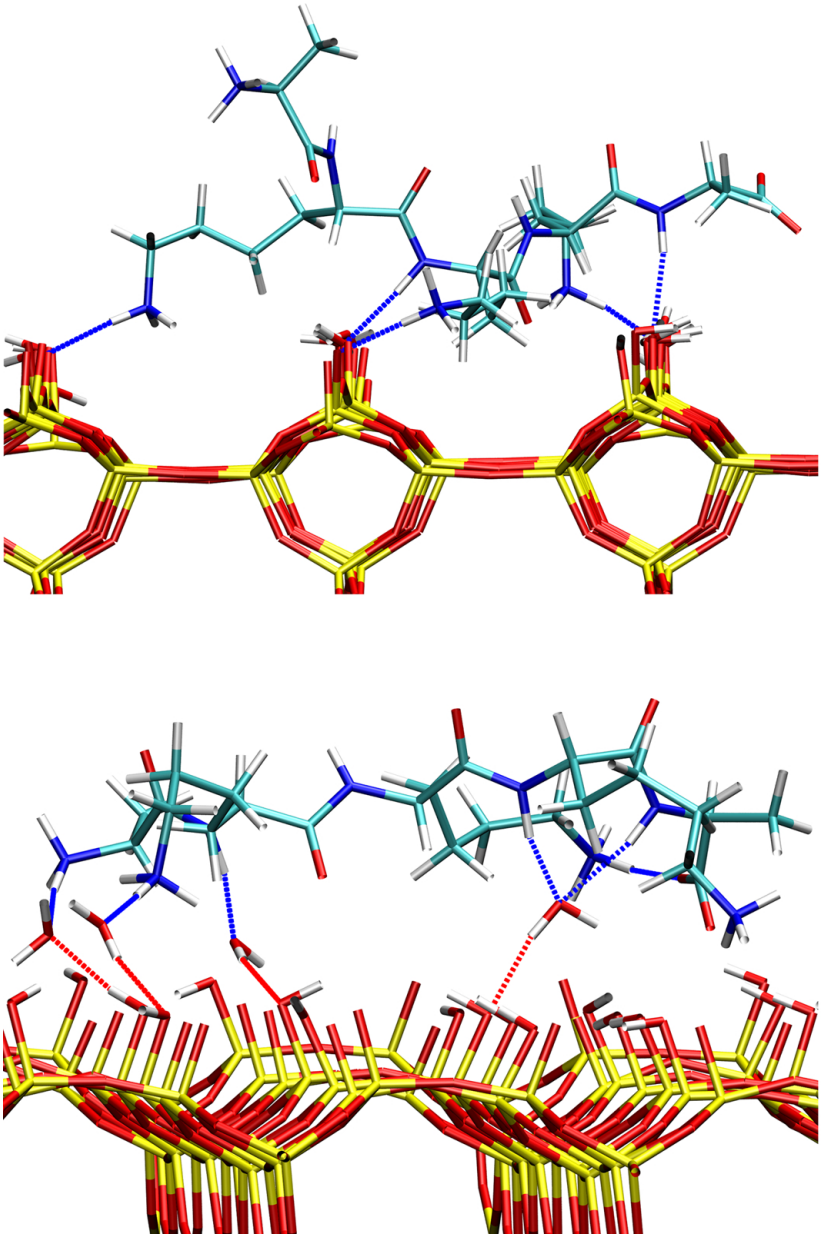

Figure 6: Peptide - silica structures exhibiting strong direct (top) or indirect (bottom) hydrogen bonding. Only water molecules involved in hydrogen bonding are shown.

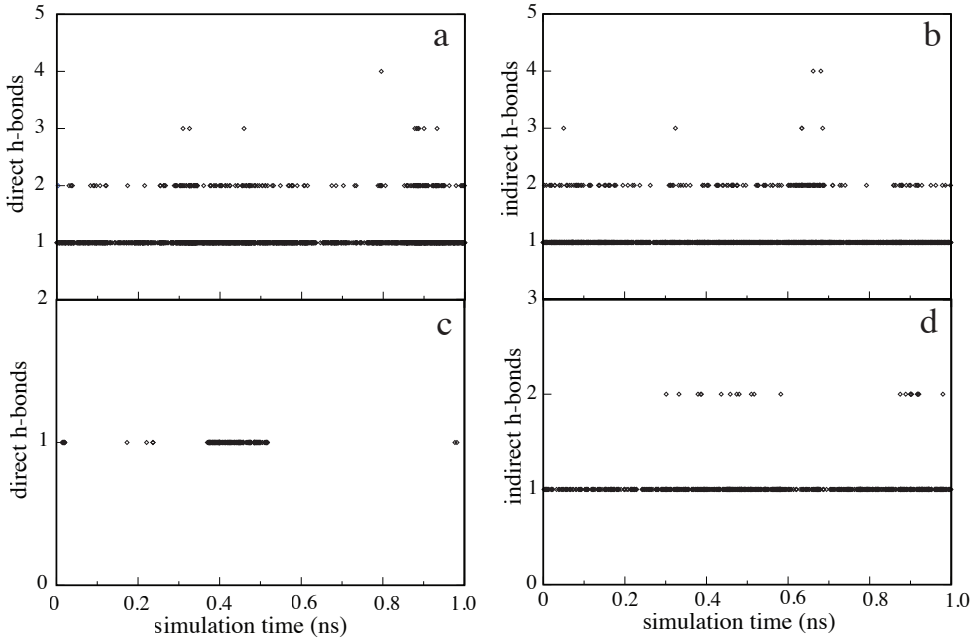

Figure 7: Typical numbers of direct (left side) or indirect (right side) hydrogen bonds during a trajectory.

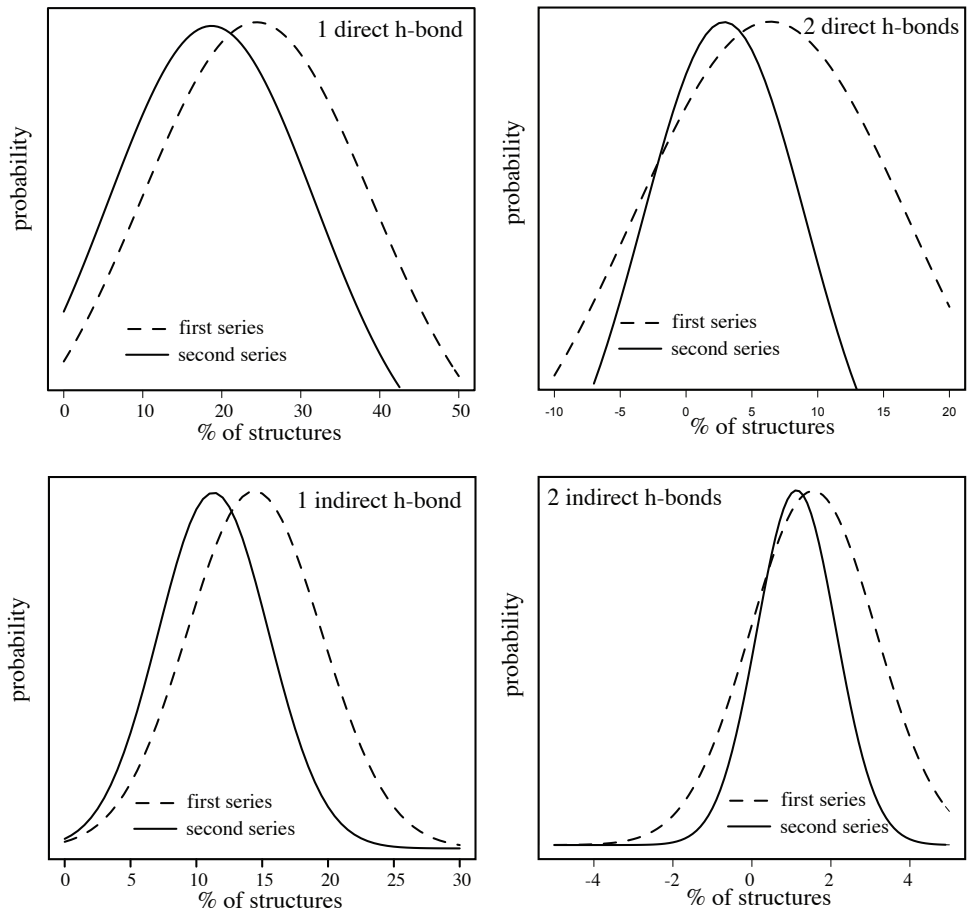

Figure 8: Probability distribution for one or two direct or indirect hydrogen bonds after 1 and 20 ns of equilibration.

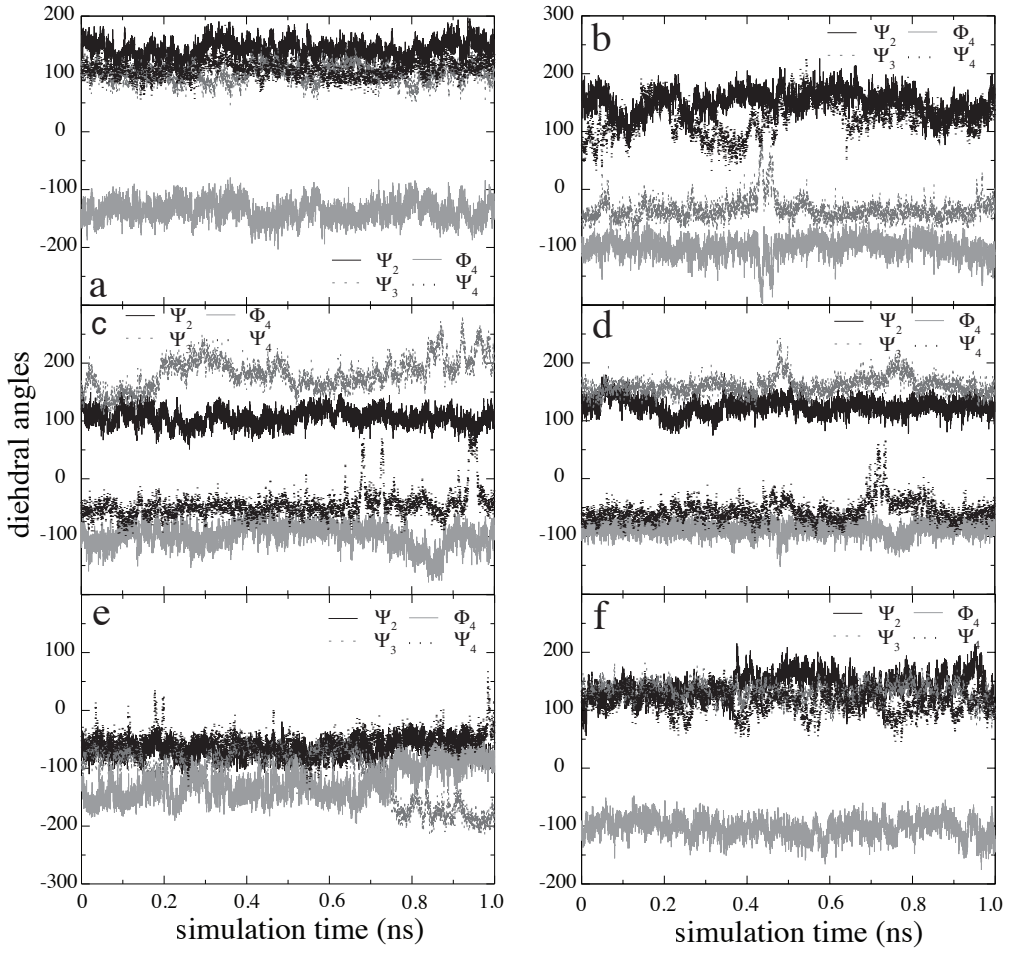

Figure 9: Time progression of selected dihedral angles. Ψ_2: black thick, Ψ_3: grey dashed, Φ_4: grey, Ψ_4: black dashed. a to e: simulations of adsorbed peptide-surface structures, f: simulation of the peptide in water.

Table of Contents:

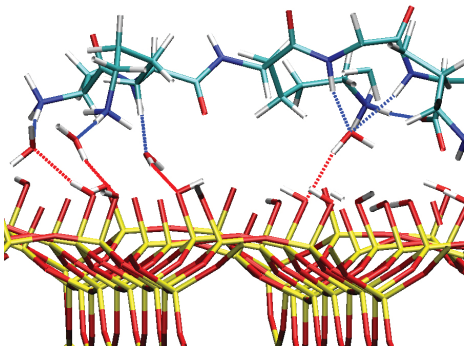

Protein-surface interactions play a crucial role in a wide field of research areas like biology, biotechnology, or pharmacology. Only recently, it has been shown that not only peptide adsorption represents an important process but also spreading and clustering of adsorbed proteins. By means of classical molecular dynamics, peptide adsorption as well as the dynamics of adsorbed peptides have been investigated in order to gain deeper insight into such processes. The picture shows a snapshot of an adsorbed peptide on a silica surface showing strong direct hydrogen bonding.